Article

Not peer-reviewed version

Development of Topical Formulations Containing 20% of Coated and Uncoated Zinc Oxide Nanoparticles: Stability Assessment and Penetration Evaluation by Reflectance Confocal Laser Microscopy

Camila Helena Ferreira Cuelho *, Georgia de Assis *, Maria Jose Vieira Fonseca, Patricia Maia Campos

Posted Date: 28 September 2023

doi: 10.20944/preprints202309.1999.v1

Keywords: Transmission electron microscopy; dynamic light scattering; franz diffusion cell; texture; rheology

Article

Development of Topical Formulations Containing 20% of Coated and Uncoated Zinc Oxide Nanoparticles: Stability Assessment and Penetration Evaluation by Reflectance Confocal Laser Microscopy

Camila Helena Ferreira Cuelho [a,*], Georgia de Assis Dias Alves [a], Maria José Vieira Fonseca [a] and Patrícia Maria Berardo Gonçalves Maia Campos [a]

[a] Department of Pharmaceutical Sciences, School of Pharmaceutical Sciences of Ribeirão Preto, University of São Paulo, Ribeirão Preto, São Paulo, Brazil.

* Correspondence: author: Georgia de Assis Dias Alves, e-mail: georgia.assis@gmail.com. Cafe Avenue without number, Ribeirão Preto, São Paulo State, Brazil. Zip Code: 14040-903. Phone: +55 (16) 3315-4726

Abstract: The introduction on Zinc oxide nanoparticles (ZnOn) in sunscreens solved the issue of poor spreadability of these formulations, which often left a white film on the skin. However, safety concerns have arisen regarding the topical application of ZnOn. Some studies employed commercial sunscreens to address the safety issues of the topical application of ZnOn; however, commercial formulations are often complex and contain a wide range of ingredients that could attenuate the potential damage caused by the ZnOn. Therefore, in this study we aimed to develop a simple stable formulation containing 20% of coated and uncoated ZnOn, characterize the formulations and the nanoparticles, and assess the skin penetration in Franz diffusion cell. The Feret's diameter for the uncoated and coated ZnOn was 137 nm and 134 nm, respectively. For the uncoated ZnOn the hydrodynamic size in water was 368 nm and for the coated ZnOn, the average hydrodynamic size in ethyl acetate was 135 nm. The incorporation of ZnOn led to formulations more consistent and easier to spread, as suggested by the lower work of shear and higher values of firmness, cohesiveness, consistency and index of viscosity compared with the vehicle. The stability assessment at 45ºC suggested that the formulations containing the ZnOn were stable for 30 days and the vehicle was stable for 90 days. The assessment of the skin penetration by reflectance confocal laser microscopy indicated that the ZnOn did not permeate into the deepest layers of the skin, but accumulated on the skin furrows, hair and hair follicle.

Keywords: Transmission electron microscopy; dynamic light scattering; franz diffusion cell; texture; rheology

1. Introduction

Nanotechnology is defined as the "the design, characterization, production and application of structures, devices and systems by controlling shape and size at the nanoscale (<100 nm)" (1). The market currently presents a wide variety of sunscreen formulations because of the increase in the demand for photoprotective agents. Sunscreens can be classified into two: physical sunscreens (inorganic filters) and chemical sunscreens (organic filters). The mechanism of physical sunscreens is reflect or scatter the UV light and thereby prevent the absorption of UV light into the skin. The decrease in the size of the particles results in less skin whitening and improved UV reflectance and scattering (2). Titanium dioxide and Zinc Oxide (ZnO) are the only inorganic filters approved for sunscreen use (3).

Formulations with inorganic filters had a poor cosmetic appearance secondary to poor dispersive qualities, leaving a white or opaque film on the skin and a grainy after-feel. Therefore, these sunscreens had inconsistent and insufficient application of product, hindering wide acceptance by the public. The texture and aesthetic problem associated with sunscreens containing titanium dioxide and ZnO have largely been solved by the introduction of nanotechnology (3).

 doi:10.20944/preprints202309.1999.v1

Consumers take aesthetic into consideration when choosing a sunscreen, and nanoparticulate formulations are often preferred over microparticulate ones because they are transparent, due to reduced light scattering (4); however, there is rising concern about the safety implications of these nanomaterials (3).

Some public advocacy groups have questioned the safety of nanoparticulate-based sunscreens, and a 2017 National Sun Protection Survey by Cancer Council Australia found that only 55% of Australians believed it was safe to use sunscreen every day, down from 61% in 2014 (5).

Zinc oxide nanoparticles (ZnOn) have been shown to have more pronounced adverse effects on keratinocytes than titanium dioxide (6). An example of the toxic effect that nanoparticles may display is the disruption of the mitochondrial function, which leads to the production of reactive oxygen species and activates the oxidative stress-mediated signaling cascade. The production of reactive oxygen species can have detrimental effects on the mitochondrial genome, disturb cell-cycle distribution, induce oxidative DNA damage and loss of normal cell morphology, ultimately leading to cell death and carcinogenesis (1, 6). In addition, it has been demonstrated that ZnOn possess a genotoxic potential in human epidermal cells, depleting glutathione, catalase and superoxide dismutase (7).

The characterization of the nanoparticles is imperative to correlate it to the biological responses observed (1). Substances that are too large for penetration such as particles may be entrapped within the hair follicles. Within the hair follicles, the sebaceous gland, the bulge and the hair follicle infundibulum have been recently defined as target sites of interest. The bulge region is the host of the epithelial stem cells providing a high proliferative capacity and multipotency. The hair follicle infundibulum is a further region of interest as the lower infundibulum provides an interrupted barrier with increased permeability. (8).

Many studies have focused on the characterization of the nanoparticles (9-11) and more recent studies have tried to address the safety issues of the topical application of ZnOn (5, 12). Frequently, the studies solubilize the ZnOn in caprylic/capric triglycerides (5, 13-15). Some characterization studies employed commercial sunscreens containing ZnOn for the analysis (16, 17); however, commercial formulations are often complex and contain a wide range of ingredients, like synthetic and natural antioxidants, that could attenuate the potential damage caused by the ZnOn. Therefore, it is more relevant for studies aiming to address the safety issues of the topical application of ZnOn to develop their own formulations. As there are sunscreens in the market with 20% of ZnOn (17), in this study, we aimed to develop a simple stable formulation containing 20% of coated and uncoated ZnOn, characterize the formulations and the nanoparticles, and assess the skin penetration in Franz diffusion cell.

2. Materials and methods

2.1. Materials

Chemicals and reagents were obtained from the following commercial sources: Cetyl Alcohol (and) Glyceryl Stearate (and) PEG-75 Stearate (and) Ceteth-20 (and) Steareth-20 was acquired from Gattefossé (Lyon, France), Lanolin was purchased from Sigma-Aldrich (St. Louis, MO, USA), Caprylic/ Capric Triglycerides was acquired from Croda Chemicals (UK), Butilenglycol, Glycerin was purchased from Fragon (São Paulo, SP, Brazil), Benzyl Alcohol (and) Xylitol (and) Caprylic Acid was acquired from Chemyunion (São Paulo, Brazil), Phenoxyethanol was purchased from Sigma-Aldrich (St. Louis, MO, USA), and the uncoated nanoparticles and the nanoparticles coated with triethoxycaprylylsilane were purchased from BASF (Ludwigshafen, Germany).

2.2. Characterization of ZnOn

The uncoated and coated (triethoxycaprylylsilane) ZnOn were characterized concerning its zeta potential, size and morphology.

2.2.1. Evaluation of the nanoparticles' size and morphology using microscopy

Preprints (www.preprints.org) | NOT PEER-REVIEWED | Posted: 28 September 2023 doi:10.20944/preprints202309.1999.v1

The morphology of the ZnOn was assessed by Scanning Electron Microscopy (SEM) and Transmission electron microscopy (TEM) and the size was assessed by TEM.

Samples for TEM analysis were prepared by dispersing 0.1g of ZnOn in 10mL of deionized water. The samples were diluted 8X and then deposited onto the inner meshed surface of carbon-coated TEM Cu-grids. After a few seconds, the excess of the dispersion was removed with a filter paper and the grids were dried overnight in the dark at 25 °C. The JEOL JEM-1000CX II (Tokyo, Japan) transmission electron microscope operating at 100 kV was employed for the analysis. The min (width) and max (length) feret's diameter were assessed in approx. 100 particles for each sample with the aid of the ImageJ/Fiji program.

Samples for SEM were prepared by sprinkling approx. 5 mg of ZnOn powder over adhesive conducting tape covering an SEM metal stub. The nanoparticles were coated with gold using a BALTEC SCD 050 sputter coater. Sputtering was conducted under vacuum while the passing gas was argon. The coating deposition time was 120 s at a plate current of 100 mA, giving a coating thickness of approximately 10 nm. The JEOL JSM 6610LV (Tokyo, Japan) scanning electron microscope operating at 20 kV was employed for the analysis.

2.2.2. Determination of the hydrodynamic size by Dynamic light scattering (DLS)

The z-average hydrodynamic particle diameter was obtained using a Zetasizer Nano ZS (Malvern Panalytical) with a detection of 90°. Disposable polystyrene cuvettes were used for determinations using water as dispersant and the DIP cell was used for the determinations using ethyl acetate. The determinations were a modification of previously reported protocols (10, 18) at a temperature of 25 °C. The following dilutions were tested aiming to optimize the detection: coated ZnOn were diluted ethyl acetate (2 mg/ 10 mL; diluted 10 fold), uncoated ZnOn were diluted in deionized water (2 mg/40mL; 1 hour ultrassonic bath or 10 mg/6 ml deionized water; ultrasonic bath for 30 min) and the coated ZnOn were diluted in deionized water (2 mg/40mL; 1 hour ultrassonic bath or 10 mg/3 ml deionized water; ultrasonic bath for 30 min, diluted 2 times).

2.2.3. Determination of the zeta potential

The zeta potential was assessed by laser Doppler electrophoresis using a Zetasizer Nano ZS (Malvern Panalytical). The uncoated ZnOn were dispersed in deionized water at 10 mg/ 6 mL following a 20 fold dilution and the coated ZnOn were dispersed in deionized water at 10 mg/ 3 mL following a 2 fold dilution. The measurements were calculated by the Helmholtz–Smoluchowski equation.

2.3. Development and characterization of the topical formulations

The formulations were prepared by heating the oil phase at 50ºC and the aqueous phase at 75ºC following spontaneously emulsification by adding the oil phase in the aqueous phase and stirring for 40 min at 800 rpm. The coated ZnOn was added in the oil phase and the uncoated ZnOn was added in the aqueous phase. Table 1 presents the composition of the topical formulations. The preservative 1 was chosen as a replacement of the controversial preservatives and chemically it consists of a 100% biodegradable ester from vegetal origin. Preservative 2 was added to broaden the effectiveness against fungi. The formulations were characterized by their texture, hardness and zeta potential.

Table 1. Composition of the formulations containing ZnOn (percentage w/w).

Component	V (%)	C (%)	UC (%)
Self emulsifying base	6	6	6
Lanolin	3	3	3

Caprylic/ Capric Triglycerides	6	6	6
Butilenglycol	3	3	3
Glycerin	4	4	4
Mcllavaine buffer (pH 5.0)	q.s.p	q.s.p	q.s.p
Preservative 1	0.8	0.8	0.8
Preservative 2	0.25	0.25	0.25
Coated ZnOn	-	20	-
Uncoated ZnOn	-	-	20

Self emulsifying base: Cetyl Alcohol (and) Glyceryl Stearate (and) PEG-75 Stearate (and) Ceteth-20 (and) Steareth-20. Preservative 1: Benzyl Alcohol (and) Xylitol (and) Caprylic Acid. Preservative 2: Phenoxyethanol. Coated ZnOn: ZnOn + triethoxycaprylylsilane.

2.3.1. Determination of zeta potential of the formulations

The formulations were suspended in water (50 mg/ 3ml, followed by 50X dilution) and the zeta potential was evaluated by laser Doppler electrophoresis in the Zetasizer Nano ZS (Malvern Panalytical).

2.3.2. Texture analyses

The texture analysis was performed using a TA.XT plus Texture Analyzer (Stable Microsystems, United Kingdom) equipped with two probes: TTC Spreadability rig HDP/SR and Back Extrusion rig A/BE 35 mm at room temperature. The work of shear was obtained from the area under the positive curve (19). The probe conditions were return distance 25 mm, return speed 20 mm s^{-1} and contact force 30 g. The firmness was obtained from the maximum value of the positive curve, the consistency from the area under the positive curve, the cohesiveness from the maximum value of the negative curve and the index of viscosity from the area under the negative curve (19). For these parameters, the formulations were loaded in containers with 50 mm of diameter (125 mL). The return distance used was 100 mm, the return speed was 20 mm s^{-1} and the contact force was 30 g. The data obtained from the negative curve were analyzed as absolute values.

2.3.3. Hardness analysis

The texture analysis was performed using a TA.XT plus Texture Analyzer (Stable Microsystems, United Kingdom). The method was conducted under the following conditions: pre-test speed of 2 mm/sec; test speed of 1mm/sec; 1% of rupture test distance; force of 0.01 kg; automatic trigger force of 0.015 kg and platform distance of 10 mm. The following parameters were calculated as mean of five measurements: hardness (g); compressibility (mm2); tackiness (g) and elasticity (cm).

 doi:10.20944/preprints202309.1999.v1

2.4. Stability Evaluation

The stability study evaluated the physical, functional and structural stability of the formulations kept at 45°C ± 2°C / 75% RH ± 5% RH for 90 days. The analyzes were performed at 0, 7, 15, 30, 60, and 90 days.

2.4.1. Functional stability

The functional stability was evaluated spectroscopically by the ability of the formulations to reflect or disperse the radiation. The formulations were applied (0.2 mg/cm^2) onto the surface of the quartz cuvettes. The cuvettes were kept in the dark for 15 minutes. Then, the reading solution was added to the cuvettes and the reflected or dispersed light was read from 280 to 400 nm. The reading solution was prepared by adding 1.25 mL of a 0.01% quercetin solution and 1 mL of a 6% aluminum chloride solution to 22.5 mL of ethanol. The area under the curve was calculated in the GraphPad Prism® software.

2.4.2. Structural stability

The microscopic analyses were performed on the Zeiss Axiovert 40 inverted microscope and the images were processed in the Axiovision Rel. 4.8.2 software (Carl Zeiss, Jena, Germany). The hydrodynamic size of the formulations (50mg / 3ml, followed by 50X dilution) was evaluated by DLS in polystyrene cuvettes with the aid of Zetasizer Nano ZS (Malvern Panalytical) with a detection angle of 90°.

2.4.3. Physical stability- rheological assessment

The rheological behavior was assessed at 25ºC on the Brookfield DV-III digital cone/plate rheometer with a 4mm GAP and the CP25 spindle. The total analysis time was 80 seconds for the ascending and descending curves and the rotation speed varied from 0 to 4 rpm. The RHEOCALC software version V 1.01 was used to obtain the apparent viscosity values. The flow index, thixotropy (hysteresis area) and consistency index were calculated using the the Origin 8.0 software.

2.5. Assessment of the microbiological quality and antimicrobial efficiency testing

The microbiological quality of the vehicle and the formulations containing ZnOn was assessed in accordance with the microbiological test described in U.S. Pharmacopeia (20).

The efficacy of the preservatives in the formulations was evaluated against *Staphylococcus aureus* (ATCC 6538), *Pseudomonas aeruginosa* (ATCC 9027) and *Escherichia coli* (ATCC 10536) and *Candida albican*s (ATCC 11006) according to the procedure and acceptability criteria described in the in U.S. Pharmacopeia (20).

2.6. Skin penetration assessment

The skin penetration assessment was carried out in a Franz-type diffusion cell as follows: the receptor compartment was filled with 20 mM isotonic phosphate buffer (pH 7.4) with 0.5% (v/v) polyoxyethylene (20) sorbitan monolaurate. The porcine skin was clamped between the donor and the receptor chambers with the stratum corneum facing upward and the dermis in contact with the receptor medium. Samples of 2 mg/cm^2 of the formulations were placed on the epidermis in the donor chamber. The diffusion cells were incubated at 32°C, and the receptor medium was stirred with a rotating Teflon-coated magnet for 12 hours. The skins were analyzed qualitatively using the Reflectance Confocal Laser Microscope Vivascope® 150 (Lucid, Rochester, NY).

2.7. Statistical analysis

The normality was evaluated with the aid of the Origin 8.0 software and the statistical analyses were carried out on GraphPad Prism® software. The normally distributed data underwent the analysis of variance followed by the Bonferroni test. The data that was not drawn from a normal

 doi:10.20944/preprints202309.1999.v1

distribution underwent the Kruskal-Wallis test followed by the Dunn's multiple comparison test. The values of $p < 0.05$ were statistically indicative of difference between the data in question under a 95% confidence interval.

3. Results and Discussion

3.1. Characterization of ZnOn

The International Organization for Standardization emphasizes that the physicochemical characterization of nanomaterials is critical for the identification of test materials before toxicological assessment (21). Therefore, the characterization of ZnOn was carried out before the development of the topical formulation.

The SEM evaluation showed that the ZnOn powders were highly agglomerated and aggregated, as visible in the micrographs (Figure 1 a, b). The assessment of the morphology presented nanoparticles with rod, cubic, tetragonal, hexagonal and orthorhombic morphologies for both samples. In some cases, nanoparticles may enter the cell after binding to the receptor target. Once bound, several factors can dictate the behavior of nanomaterials at the nano-bio interface, e.g., the nanoparticle's shape may influences uptake into cells. For nanoparticles with size larger than 100 nm, rods show the highest uptake, followed by spheres, cylinders, and cubes (1). In this study it was observed a high incidence of rod-shaped nanoparticles in the coated and uncoated ZnOn; therefore, the cell uptake could be increased.

The assessment of the size of the uncoated (Figure 1 c) and coated (Figure 1 d) ZnOn by TEM varied from 55 to 413 nm and from 39 to 456 nm, respectively. For titanium dioxide, which is another inorganic filter, the nanoparticles with 30 nm have been demonstrated to induce the highest generation of reactive oxygen species (1). The presence of small sized nanoparticles in the uncoated and coated samples could result in the cell uptake of these nanoparticles, which could lead to cell damage.

The average of the max feret's diameter for the uncoated and coated ZnOn was 137 nm and 134 nm, respectively (Figure 2 a, b). For the uncoated and coated ZnOn, 86.2% and 88.8% of the nanoparticles exhibited size lower than 200 nm, respectively, which indicates that although the ZnOn presented a large size distribution, the majority of the nanoparticles were encompassed in the group with size lower than 200 nm. The ratio of max per min feret's diameter varied from 1.1 to 9.9 and from 1.1. to 5.6 for the coated and uncoated ZnOn, respectively. For the uncoated and coated ZnOn, 53.6% and 75.5% presented ratio higher than 2, respectively, which is characteristic of tetragonal, hexagonal and orthorhombic and long rod-shaped nanoparticles (18). For the coated ZnOn, the size of all the nanoparticles with ration lower than 2 was equal or lower than 200 nm. For the uncoated ZnOn, 94.7% of the nanoparticles with ration lower than 2 exhibited size lower than 200 nm. For the uncoated and coated ZnOn, 81.8% and 75.7% of the nanoparticle with ration higher than 2 exhibited size higher than 100 nm, respectively, which is characteristic of cubic and short rod-shaped nanoparticles (18).

 doi:10.20944/preprints202309.1999.v1

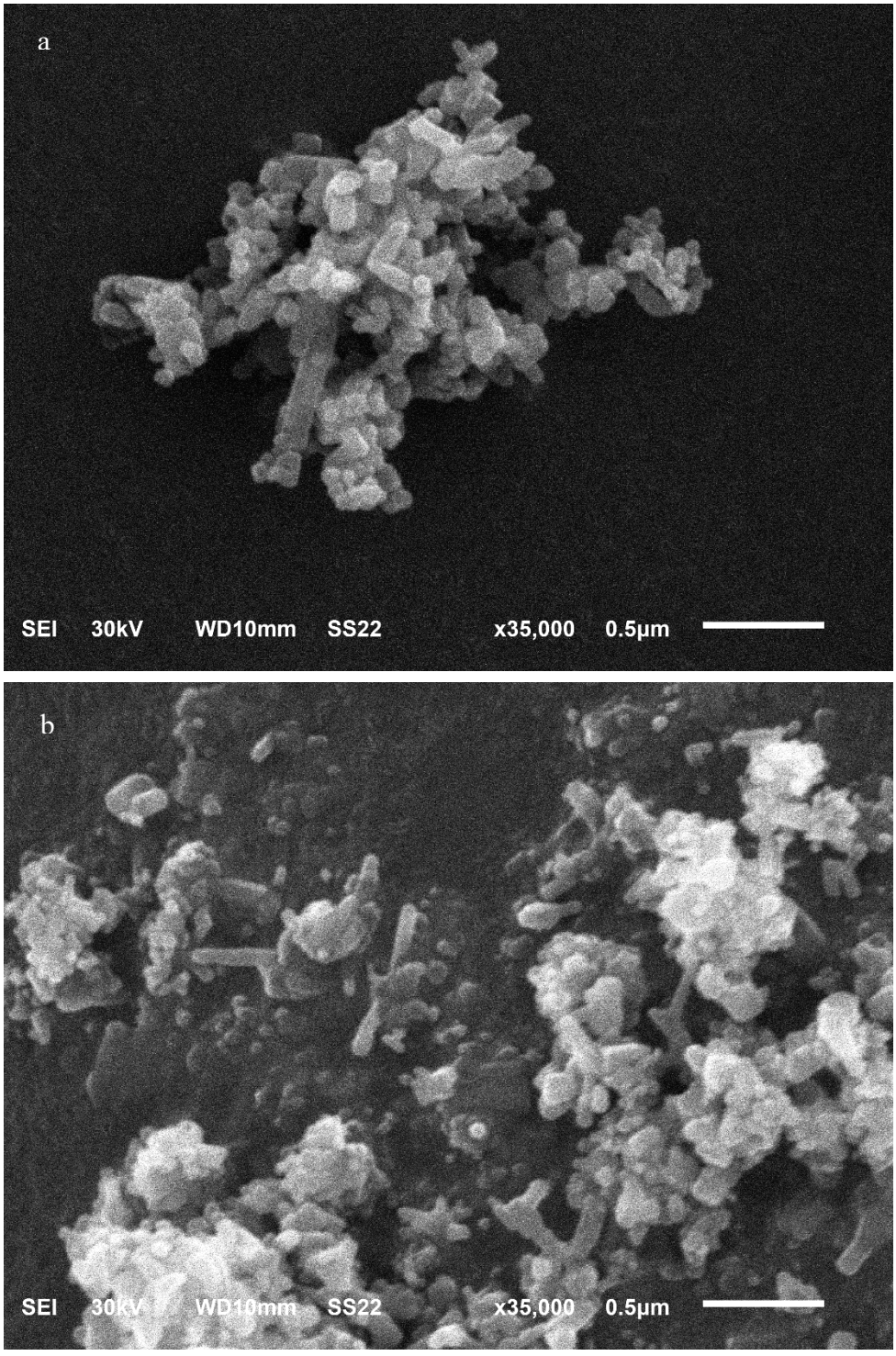

 doi:10.20944/preprints202309.1999.v1

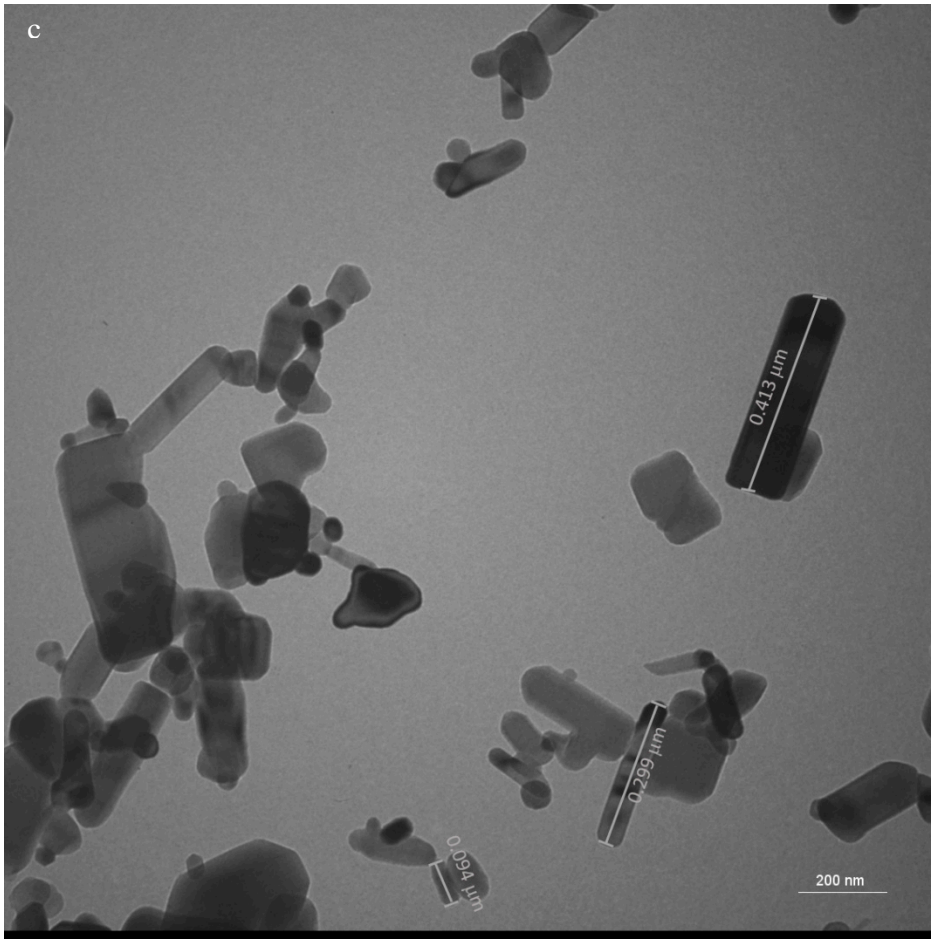

Preprints (www.preprints.org) | NOT PEER-REVIEWED | Posted: 28 September 2023 doi:10.20944/preprints202309.1999.v1

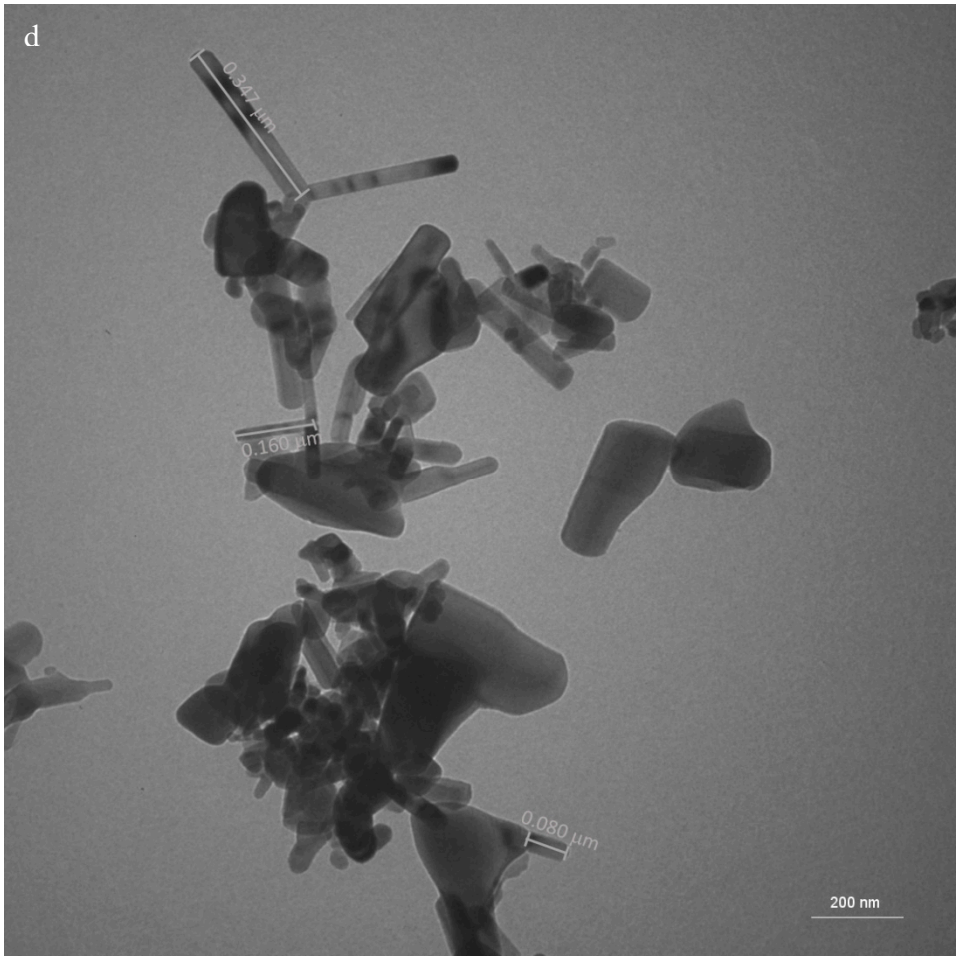

Figure 1. SEM and TEM images of of the uncoated (a,c) and coated (b,d) ZnOn.

A previous study employed the protocol used in this study for the hydrodynamic particle size determination using DLS (10 mg/3 ml deionized water; ultrasonic bath for 10s). They obtained an average hydrodynamic size and PDI of 340 nm, 192 nm and 0.2, 0.2 for the uncoated and coated ZnOn, respectively (10). In this study, the average hydrodynamic size and PDI for the coated ZnOn under these conditions were 371 nm and 0.295, respectively. The hydrodynamic size decreased for 282 nm when the samples were kept in an ultrasonic bath for 1 hour; however, the PDI increased for 0.332.

For the uncoated ZnOn, 3 mL of deionized water was not enough to suspend 10 mg of the nanoparticles, therefore, the sample were suspended in 6 mL of deionized water and were diluted 2 fold to achieve a hydrodynamic size and PDI of 368 and 0.259, respectively (figure 2 c). This concentration was the best result we obtained for the uncoated ZnOn; however, the mean hydrodynamic size is considerably higher than the mean feret's diameter (137 nm), which suggests that DLS is not an appropriate methodology to assessment the size of the uncoated ZnOn under the tested conditions.

Other study encountered better results with the samples in the concentration 50 mg/L (18). Their results of hydrodynamic sizes and PDI for the uncoated and coated ZnOn was 275 nm, 253 nm and 0.145, 0.401, respectively. We tested this concentration (2 mg/40mL; 1 hour ultrassonic bath) and obtained similar results of hydrodynamic size and PDI for the coated ZnOn, respectively, 258 nm and 0.238. However, for the uncoated ZnOn the hydrodynamic size was remarkably higher, 962 nm (PDI: 0.258), which indicates substantial agglomeration

The hydrodynamic diameter found for the coated and uncoated ZnOn was larger than the feret's diameters measured by TEM. That is often the case for several nanoparticles because when a dispersed particle moves through a liquid medium an electric dipole layer, which is often thin,

Preprints (www.preprints.org) | NOT PEER-REVIEWED | Posted: 28 September 2023 doi:10.20944/preprints202309.1999.v1

adheres to its surface. Thus, the hydrodynamic diameter gives us information of the solvent layer attached to the particle as it moves under the influence of Brownian motion (22).

Aiming to reduce the agglomeration, organic solvents were tested in order to improve the solubilization of the nanoparticles. The coated ZnOn solubilized exceedingly well in ethyl acetate. The sample was visually stable with no signs of sedimentation, which suggests that the particles were undergoing Brownian diffusional motion throughout the measurement.

The average hydrodynamic size and the PDI for the coated ZnOn in ethyl acetate (2 mg/ 10 mL; diluted 10 fold) was 135 and 0.149 respectively (figure 2 d). Although the PDI indicates a polydisperse sample (values smaller than about 0.04 are considered monodisperse) (18), this could be a characteristic of the sample, rather than an indication of the poor applicability of the technique. The size found by DLS was compatible to the feret's diameter (134nm), which suggests that opposed to what has previously been believed (10, 18), DLS is an appropriate technique for measuring the mean hydrodynamic diameter of the coated ZnOn if the nanoparticles are suspended in ethyl acetate. DLS is a technique widely used to assess hydrodynamic diameters of nanoparticle dispersions; therefore, these results are important to substantiate the use of this technique for the coated ZnOn.

The zeta potential for the coated (10 mg/ 3 mL; diluted 2 fold) and uncoated (10 mg/ 6 mL; diluted 20 fold) ZnOn in deionized water was -19.5. and 21.3, respectively. It has been discussed that the smallest agglomerate size are achieved when the nanoparticle displays a strongly charged surface. The intense charge on the surface increases the charge-charge repulsions between the particles, thus maintaining a more stable and monodisperse suspension (23). However, for the tested ZnOn, the zeta potential was high and there was still significant agglomeration. The results for the zeta potential are in agreement with other studies that show that uncoated zinc oxide nanoparticles often exhibit positive zeta potential, while the nanoparticles coated with triethoxycaprylylsilane exhibit negative zeta potential (10, 18, 23). This indicates that the coating material may be associated with the shift in the zeta potential. Moreover, it has been suggested that positively charged nanoparticles are taken by the cells at a faster rate than nanoparticles with a neutral or negative charge, (1). This suggests that the skin toxicity may be different for the two ZnOn tested.

Furthermore, the zeta potential of the coated ZnOn in ethyl acetate (2 mg/ 10 mL; diluted 10 fold) was 0.0657. It has been suggested that a hypothetical model nanoparticle exhibits the largest agglomerate size at the point where its zeta potential is 0 mV (23). However, in ethyl acetate the zeta potential was close to zero and there was no significant agglomeration, which is possibly related to the low conductivity of the non aqueous dispersant.

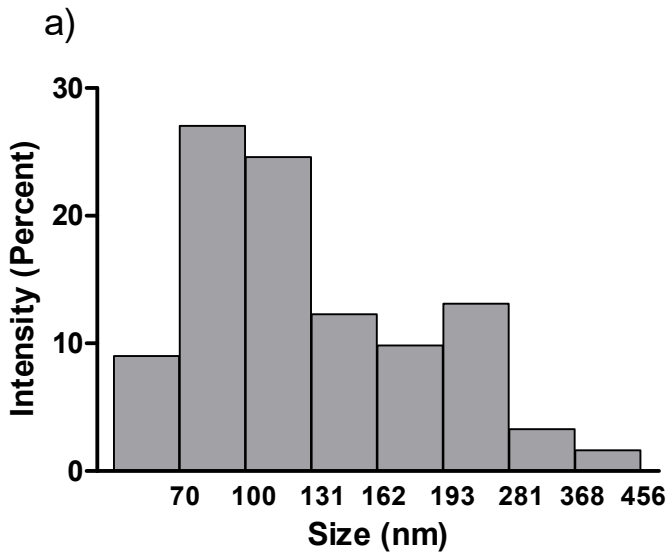

Preprints (www.preprints.org) | NOT PEER-REVIEWED | Posted: 28 September 2023 doi:10.20944/preprints202309.1999.v1

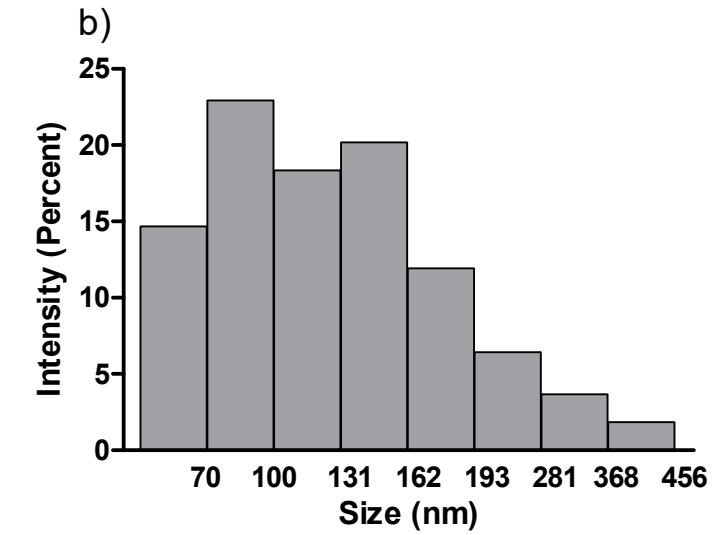

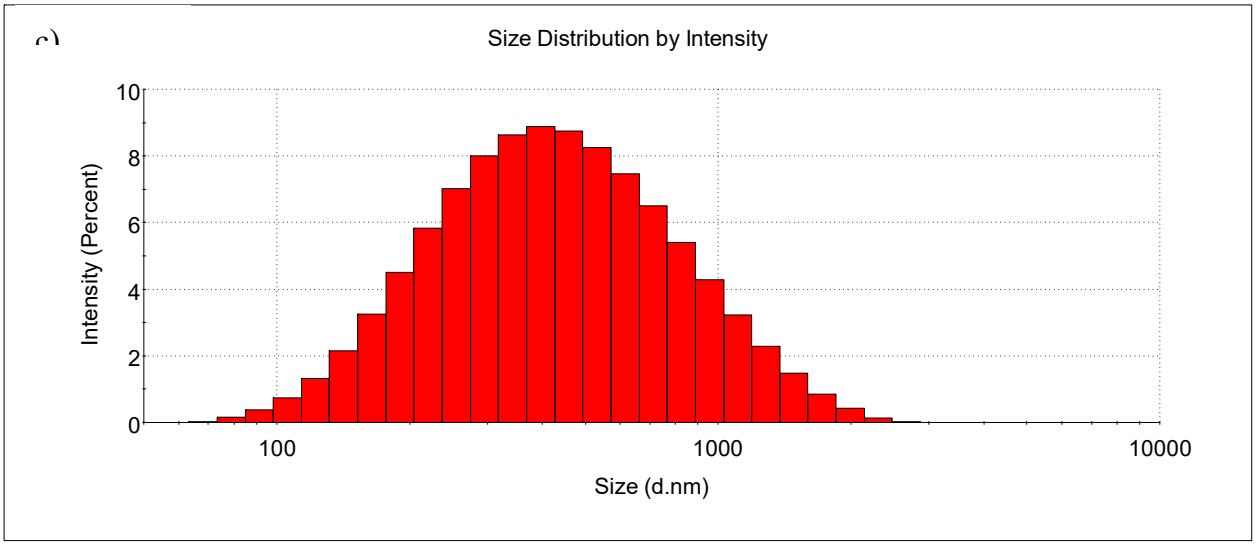

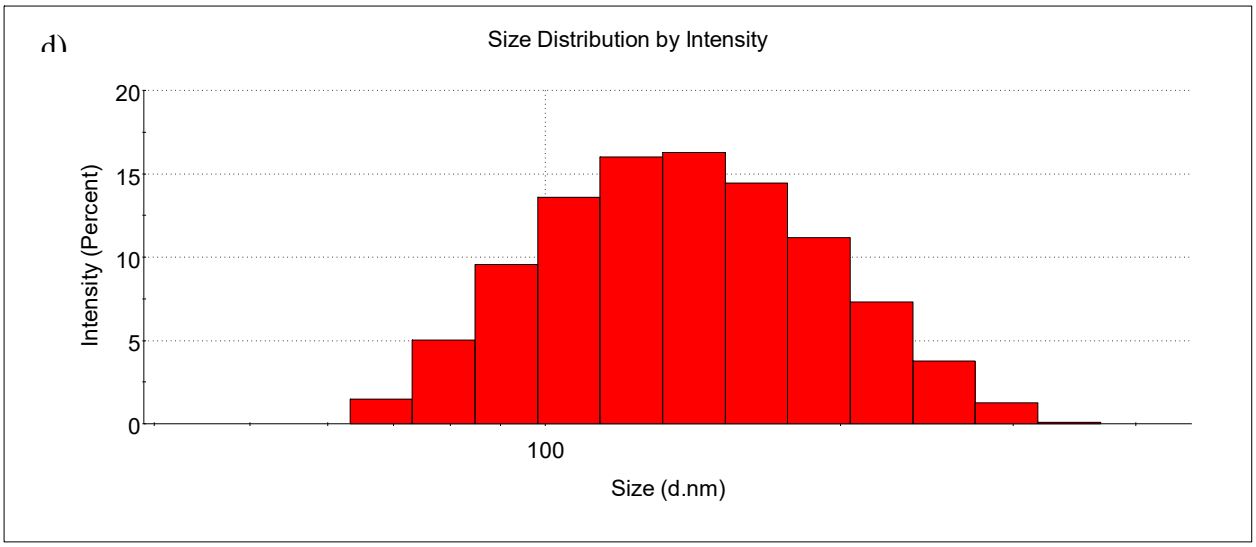

Figure 2. Size distribution histograms by TEM and DLS of the uncoated (a,c) and coated Zinc Oxide nanoparticles (b,d), respectively.

3.2. Development and characterization of the topical formulations

 doi:10.20944/preprints202309.1999.v1

Several formulations were tested aiming to incorporate 20% of ZnOn in the formulations. Initially the formulations were tested in water instead of buffer to avoid instability due to incompatibility. The first formulations were developed based on a previous study (24) and the main ingredients were ceteareth-20, cetearyl alcohol and a different polymers, besides emollients and humectants. Formulations employing a non ionic self emulsifying base (Cetearyl Alcohol, polyoxyethylene derivative of a fatty acid ester of sorbitan) and an anionic self emulsifying base (Mineral Oil, Isopropyl Palmitate, Trilaureth-4 Phosphate, Rapseed Oil Sorbitol Esters and Ammonium Acryloyldimethyltaurate/VP Copolymer) were also tested. The amount of 20% of ZnOn solubilized in Caprylic Capric Triglycerides was firstly incorporation in the formulation in the end of the process of preparation, which resulted in immediate phase separation. Therefore, the ZnOn were then incorporated either in the aqueous (uncoated ZnOn) or oil phases (coated ZnOn). None of the above mentioned formulations were stable and in up to 5 minutes they exhibited a distinguished appearance: the formulations presented characteristic white color and were fragmented in small granules with medium consistency, suggesting the consumption of the water.

The formulation with the non-ionic self emulsifying base presented in Table 1 resulted in an initially stable formulation. The formulation was firstly prepared in water and latter prepared in buffer to avoid pH variation. It was observed that the formulation prepared in buffer was more consistent than the one prepared in water. Moreover, it was observed that the addition of the ZnOn increased considerably the pH. Using a buffer with the pH 3.5, the vehicle pH was 4, while the pH of the formulations containing ZnOn was 8.0. Therefore, the formulations were prepared in buffer pH 5.0, which resulted in a vehicle with pH 5.5 and formulations with pH 8.0. The pH of the formulations containing ZnOn decreased up to approximately 6.1.

3.2.1. Characterization of the topical formulations

The zeta potential of the vehicle and the formulations containing the uncoated and coated ZnOn were -22 mV, -13 mV and -8 mV, respectively. It was observed that the incorporation of ZnOn decreased the zeta potential, which could destabilize the formulation.

The texture parameters showed that the work of shear of the formulations containing the ZnOn were not significantly different and were smaller than the vehicle (Figure 3). The work of shear represents the total amount of force required to perform the shear process during the texture test (25) and it is inversely related to the spreadability of the sample (26). Therefore, the formulations containing the ZnOn presented lower work of shear, which indicates that the incorporation of the nanoparticles in the vehicle led to formulations which were easier to spread.

The visual evaluation of the formulations suggested that the incorporation of ZnOn led to more consistent formulations, which was confirmed by the higher values of firmness, cohesiveness, consistency and index of viscosity for the formulations containing ZnOn compared with the vehicle (Fig. 3). Firmness represents the maximum force during the probe penetration to shear in texture test (25). This suggests that during the test, the formulations containing ZnOn endured the application of higher force than the vehicle, but less force was required for the formulations containing the ZnOn to be spread. In addition, the formulation containing the coated ZnOn presented higher texture values than the formulation containing the uncoated ZnOn but the work of shear was not statistically different. This indicates that the increase in firmness, cohesiveness, consistency and viscosity index for the formulation containing the coated ZnOn was not substantial enough to affect the spreadability of the formulation.

Thixotropy is defined as the continuous decrease of viscosity with time when flow is applied to a sample that has been previously at rest and the subsequent recovery of viscosity in time when the flow is discontinued (27). Therefore, topical formulations with a thixotropic behavior are highly desired because they deform during the application. It is interesting to obtain a thixotropy value not too high so that the product does not run on the skin after application but not a very low value, since it can result in low spreadability and non-uniform distribution on the skin (28).

The formulation containing the coated ZnOn presented significantly higher thixotropy than the vehicle and the formulation containing the uncoated ZnOn (Figure 8). Although the work of shear

 doi:10.20944/preprints202309.1999.v1

was significantly different between formulations containing ZnOn, the thixotropy suggests that the formulation containing the coated ZnOn could have better spreadability, which reinforces the results of the texture parameters. In addition, the texture and thixotropy results suggest that the coating of the nanoparticles with triethoxycaprilylsilane may have had a positive impact on the texture and spreadability of the formulation.

Elasticity is the ratio of the duration of contact with the sample between the second and first compression, which indicates the rate at which a deformed material returns to its undeformed condition after the deforming force is removed (29). As shown in Figure 4, there was no change in elasticity between the formulations developed, and the value found suggests that the formulations exhibit low elasticity compared with other topical formulations (30).

Hardness is the maximum force applied to the sample during the first compression cycle (29) and the compressibility corresponds to the area (30). The stickiness is given by the force at the maximum point in the second compression cycle. Thus, a stickier sample will require a greater force for the probe to be removed (25). The hardness, stickiness and compressibility of the formulations containing the ZnOn were higher than the vehicle (Figure 4). For these parameters, there was no significant difference between the formulations containing the ZnOn. This suggests that the incorporation of the nanoparticles led to a physical alteration in the formulation, but coating the nanoparticles with trietoxicaprilylsilane did not influence the evaluated parameters.

Preprints (www.preprints.org) | NOT PEER-REVIEWED | Posted: 28 September 2023 doi:10.20944/preprints202309.1999.v1

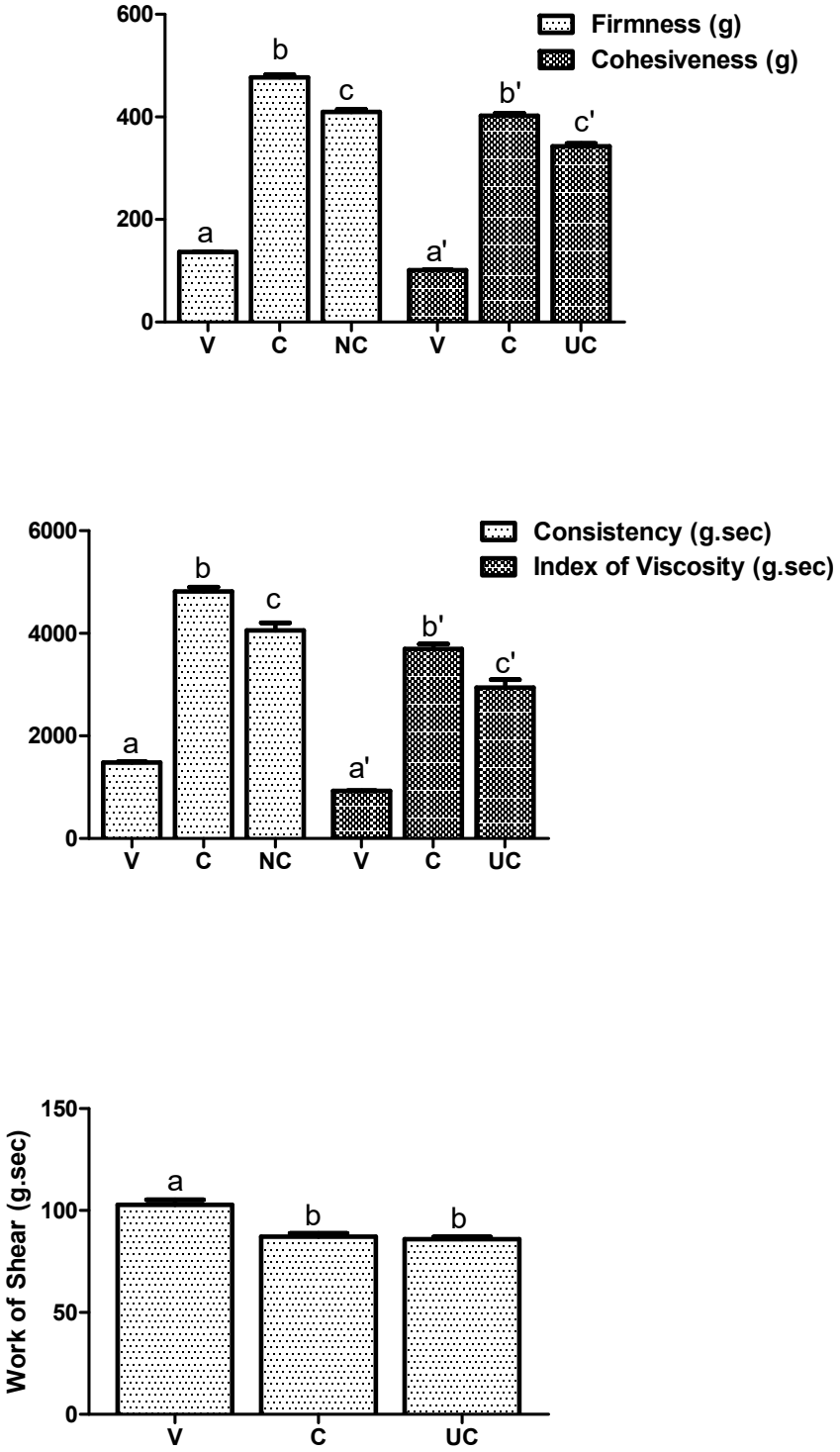

Figure 3. Texture parameters of the vehicle (V) and formulations containing the coated (C) and uncoated (UC) Zinc Oxide nanoparticle.

Preprints (www.preprints.org) | NOT PEER-REVIEWED | Posted: 28 September 2023 doi:10.20944/preprints202309.1999.v1

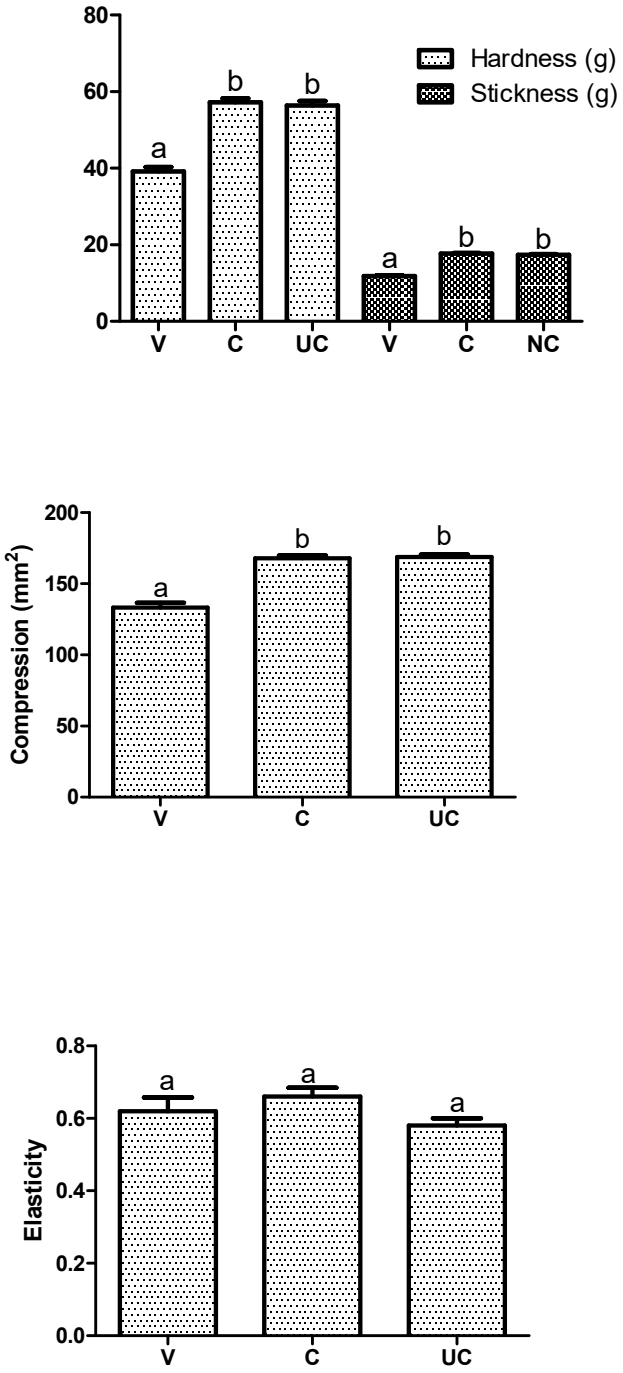

Figure 4. Hardness parameters of the vehicle (V) and formulations containing the coated (C) and uncoated (UC) Zinc Oxide nanoparticles.

3.2.2. Stability Evaluation

3.2.2.1. Functional stability

The functional stability was evaluated spectroscopically by the ability of the formulations to reflect the radiation. Figure 5 shows the absorption spectrum of the formulations developed and

 doi:10.20944/preprints202309.1999.v1

suggests that the absorption capacity of the UVA / B radiation of the formulation containing the coated ZnOn is higher than the formulation containing the uncoated ZnOn. The absorption capacity of the vehicle's UVA / B radiation was very similar to that of the control, indicating that the FPS would be close to zero.

The area under the curve of the samples at 0, 15, 30, 60 and 90 days was calculated and it was not possible to observe a change in the functional stability of the samples, since the area under the curve ranged from 61.1 to 58.9; from 39.7 to 42.8 and from 3.2 to 4.1 for formulation containing coated, uncoated and vehicle nanoparticles at 0 and 90 days, respectively. Thus, apparently the ZnOn did not undergo any process of degradation that resulted in loss of activity.

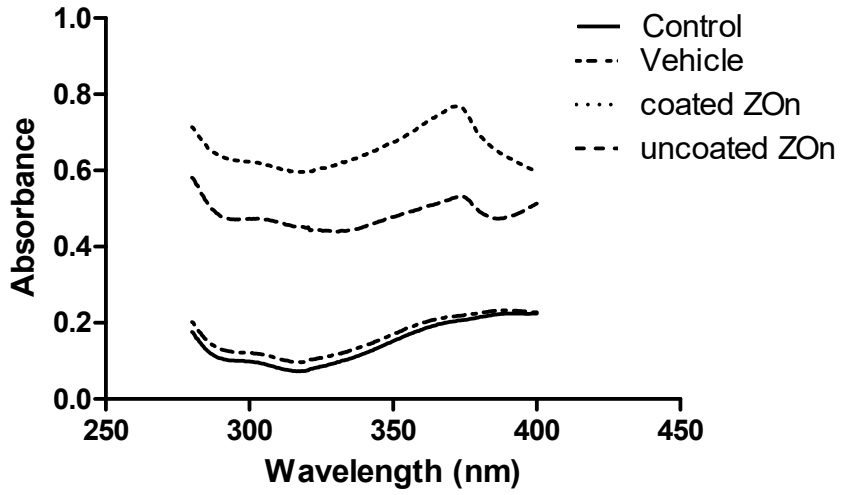

Figure 5. Absorption spectrum of the vehicle and formulations containing the coated and uncoated Zinc Oxide nanoparticles.

3.2.2.2. Structural stability

The microscopic evaluation suggested the tendency of the nanoparticles to agglomerate in the formulations. Nanoparticles have strong crystal attractions which form clustered, tightly bound aggregates. Aggregates are the smallest particles which can be found in sunscreen formulations, because the forces required to break apart aggregates are far greater than those forces encountered during production or during application onto the skin (3). The instability signs were defined as the presence of agglomerates with different characteristics than the native agglomerates of the formulation. Figure 6 shows micrographs at 0 and 90 days. It was not possible to observe any clear signs of instability for the vehicle during the study time (Figure 6 a,b). The formulations containing the uncoated ZnOn showed instability signs at day 60. The circled area points out the structures that appeared at day 60 (Fig. 6 d). For the formulations containing the coated ZnOn, signs of instability were detected at day 90 (white arrows in Figure 6 f, which are more clearly presented in Figure 7). The instability signs observed for the formulation containing the coated ZnOn had a crystalline appearance and were less evident than for the formulation containing the uncoated ZnOn.

Preprints (www.preprints.org) | NOT PEER-REVIEWED | Posted: 28 September 2023 doi:10.20944/preprints202309.1999.v1

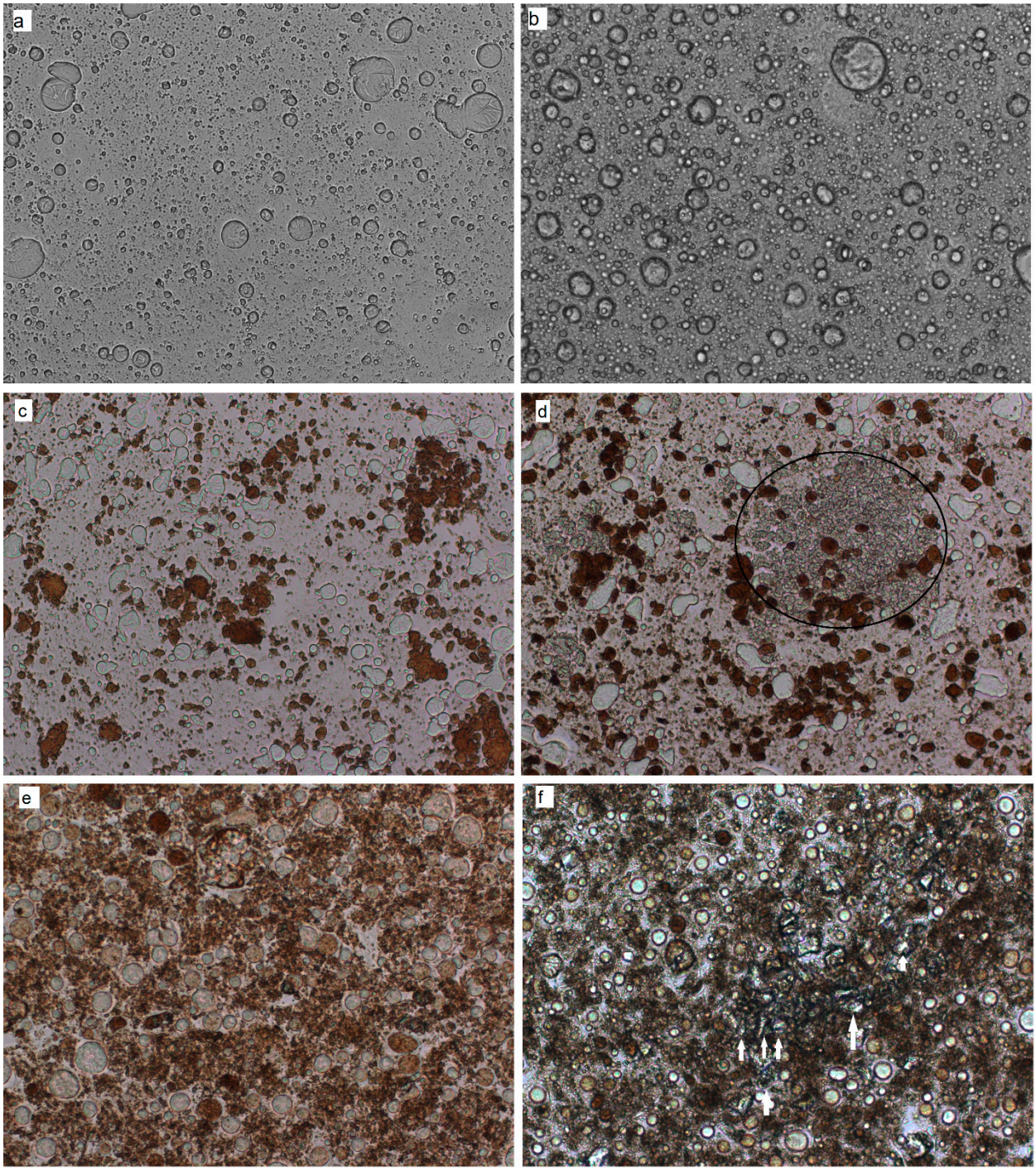

Figure 6. Micrographs of the vehicle at 0 (a) and 90 days (b), of the formulation containing the uncoated ZnOn at 30 (c) and 60 days (d) and of the formulation containing the coated ZnOn at 60 (e) and 90 days (f). Magnification of 20X. Circle (d) and arrows (f) represent the instability signs.

Preprints (www.preprints.org) | NOT PEER-REVIEWED | Posted: 28 September 2023 doi:10.20944/preprints202309.1999.v1

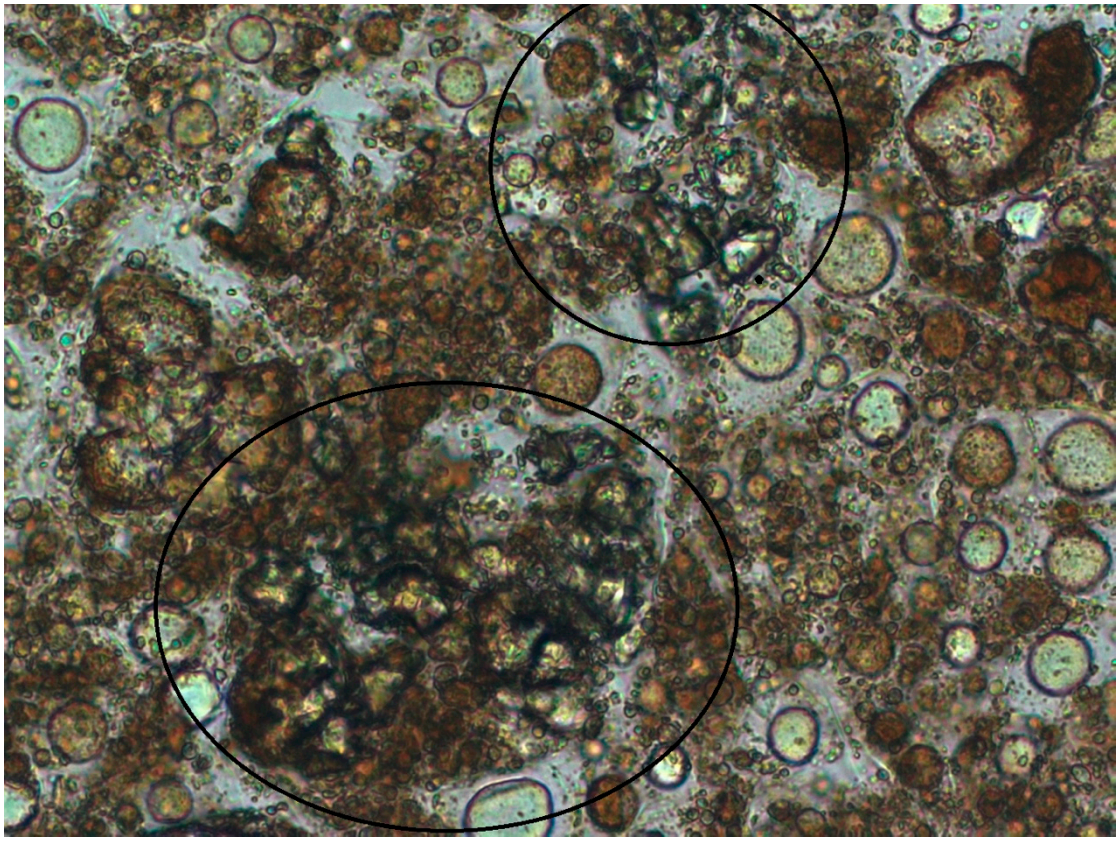

Figure 7. Micrographs of the formulation containing the coated Zinc Oxide Nanoparticles at 90 days. Magnification of 40X.

For the size evaluation by DLS, the vehicle presented a hydrodynamic size of 309.4 nm (PDI of 0.400) at time 0, indicating the presence of polydisperse nanoparticulate material in the formulation. At day 15, the size decreased to 192.9 nm (PDI of 0.308) and was maintained until the end of the study. The formulation containing the uncoated ZnOn presented a hydrodynamic size of 534 nm (PDI of 0.500) at time 0. At day 7, the size decreased to 439.2 nm (PDI: 0.417) and was maintained until the end of the study. The formulation containing the coated ZnOn presented a hydrodynamic size of 307 nm (PDI of 0.324) at time 0. At day 7, the size increased to 389 (PDI of 0.467) and was maintained until the end of the study. Evaluation of the hydrodynamic size of the formulations indicated a reorganization of the vehicle molecules from time 0 to 15 days. The same was observed for the formulations containing the ZnOn from 0 to 7 days. The DLS technique resulted in a satisfactory characterization of the formulations, but it was not able to detect instability signs possibly because the formulations were polydisperse. Moreover, the vehicle also presented nanoparticles, which might have interfered in the size determination of the ZnOn in the formulations.

3.2.2.3. Physical stability- rheological assessment

At day 60, an aqueous buildup was observed on the surface of the formulation containing the uncoated ZnOn, which is suggestive of instability. The rheological analysis confirmed the instability of the formulation and due to the lack of homogeneity, it was not possible to obtain reproducible rheograms. Thus, Supplementary Figure 1 shows the rheograms of the vehicle and the formulation containing the coated ZnOn at 0, 7, 15, 30, 60 and 90 days, while the rheograms of the formulation containing the uncoated ZnOn are presented only at 0, 7, 15 and 30 days.

The rheological characterization of the formulations and the evaluation of the viscosity, flow index, consistency index and thixotropy allow a better understanding of the physico-chemical nature of formulations in the development phase. In addition, it allows to control the quality of raw materials and finished products, to evaluate the effect of the consistency of the product on the release and skin

Preprints (www.preprints.org) | NOT PEER-REVIEWED | Posted: 28 September 2023 doi:10.20944/preprints202309.1999.v1

penetration, besides contributing to the prediction of the shelf life of the product (31). The formulations did not show significant variation in the flow index during the study time, and presented flow index lower than 1, which indicates pseudoplastic behavior. Pseudoplastic materials exhibit non-Newtonian flow and are characterized by the reduction of viscosity with the increase of the applied force (32). This behavior is the most common in cosmetic formulations and presents a characteristic film formation on the surface of the skin (33).

Figure 8 shows the variations in the hysteresis area, consistency index and minimum apparent viscosity for 90 days. For the vehicle, there was no significant variation in the parameters for 90 days. For the formulation containing the uncoated ZnOn, there was no significant difference in the parameters for 30 days. At 60 and 90 days, it was not possible to perform the rheological analysis due to the instability of the formulation, which compromised the reproducibility of the results. For the formulation containing the coated ZnOn, there was no significant difference in the parameters for 30 days. At 60 and 90 days there was a decrease in the hysteresis area, minimum apparent viscosity and consistency index compared to time 0. Therefore, the formulations and the vehicle were considered stable for 30 and 90 days, respectively.

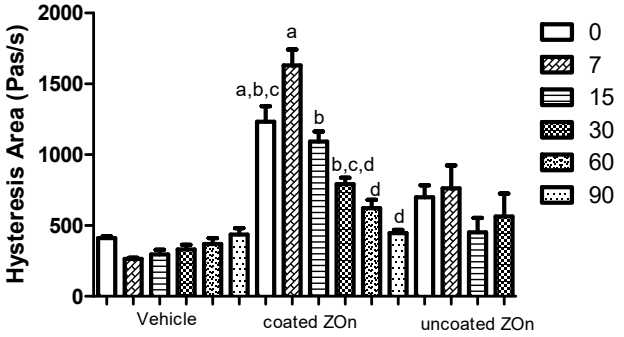

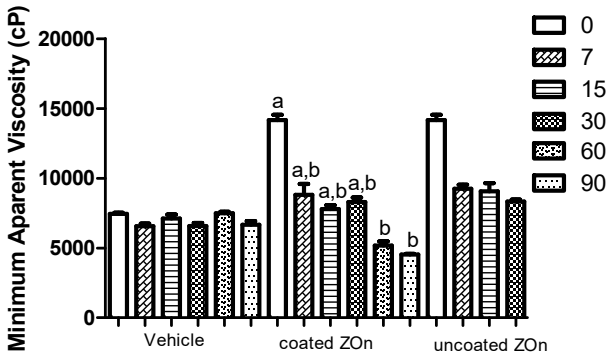

Preprints (www.preprints.org) | NOT PEER-REVIEWED | Posted: 28 September 2023 doi:10.20944/preprints202309.1999.v1

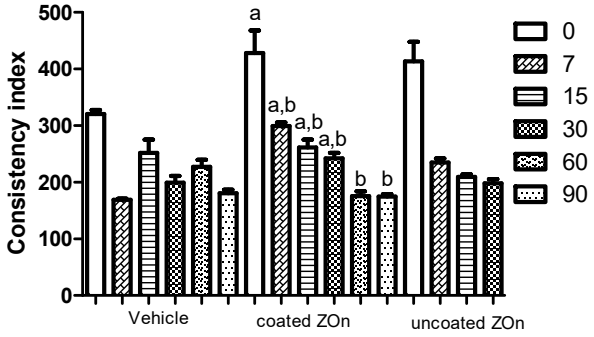

Figure 8. Minimum apparent viscosity and consistency index of the formulations incubated at 45 °C for 0, 7, 30, 60 and 90 days. Results are presented as mean ± standard error (n = 5).

3.3. Assessment of the microbiological quality and antimicrobial efficiency testing

In order to avoid skin sensitization by the preservatives, none controversial preservatives were used. Instead a biodegradable ester from vegetal origin was employed at its lower concentration of use. Therefore, it was imperative to assess the effectiveness of the preservatives used.

The total amount of aerobic microorganisms and yeasts and molds was assessed on the formulations on Trypticase soy agar and Sabouraud agar plates, respectively. Absence of colony forming units were found on the Trypticase soy agar and Sabouraud agar plates, indicating absence of microbial contamination in one gram of the formulations.

The efficiency of the preservatives, a biodegradable ester from vegetal origin and phenoxyethanol, were evaluated against *S. aureus*, *E.coli* and *P.aeruginosa* and *C. albicans*. The preservatives eliminated the microbial load added to the formulations in 14 days and the absence of growth was maintained until the day 28. These results are in accordance with the acceptance criteria for preservative established by the U.S. Pharmacopeia and indicate that the preservatives used were efficient in eliminating the microbial load that could be introduced by the consumer. Supplementary Figure 2 shows that the antimicrobial efficiency of the preservative system was similar for the vehicle and the formulations containing the ZnOn. This suggests that the ZnOn did not adsorb the preservatives or the microorganisms. If the ZnOn had adsorbed the preservatives, the antimicrobial efficiency of the formulations would be lower than the vehicle and the opposite would be observed if the ZnOn had adsorbed the microorganisms

3.4. Penetration assessment

RCM imaging is a noninvasive technique that shows nuclear and cellular-level morphology. Imaging is based on the detection of singly backscattered photons from the optical section and contrast is due to the relative variations in refractive indices and sizes of organelles and microstructure (34).

Figure 9 shows RCM images of the stratum corneum (A1, B1, C1, D1), granular layer (A2, B2, C2, D2) and hair/hair follicle (A3, B3, C3, D3) of porcine skin treated with the vehicle (B) and the formulations containing the coated (C) and uncoated (D) ZnOn. Higher reflectance in the stratum corneum was observed for the skin treated with the formulations containing the ZnOn, which suggests the presence of the ZnOn. The formulation containing the coated ZnOn evidently accumulated on the skin furrows (Figure 9. white arrows), which was not observed for the formulation containing the uncoated ZnOn.

Although the uncoated ZnOn did not show major accumulation on the skin furrows, the coated and uncoated ZnOn accumulated around the hair and in the hair follicles (Figure 9 C3 and D3). Whereas for the vehicle and the non treated skin, it was possible to observe the hair up until the

 doi:10.20944/preprints202309.1999.v1

medulla (Figure 9, A3 and B3, white arrows), a thick coat of nanoparticles covered the hair, which prevented the visualization of the inner part of the hair. Though the penetration assessment was carried out in porcine skin, the size of the porcine hair follicles corresponds approximately to the size of human terminal hair follicles. Therefore, results can be expected to be similar in human terminal hair follicles. (35).

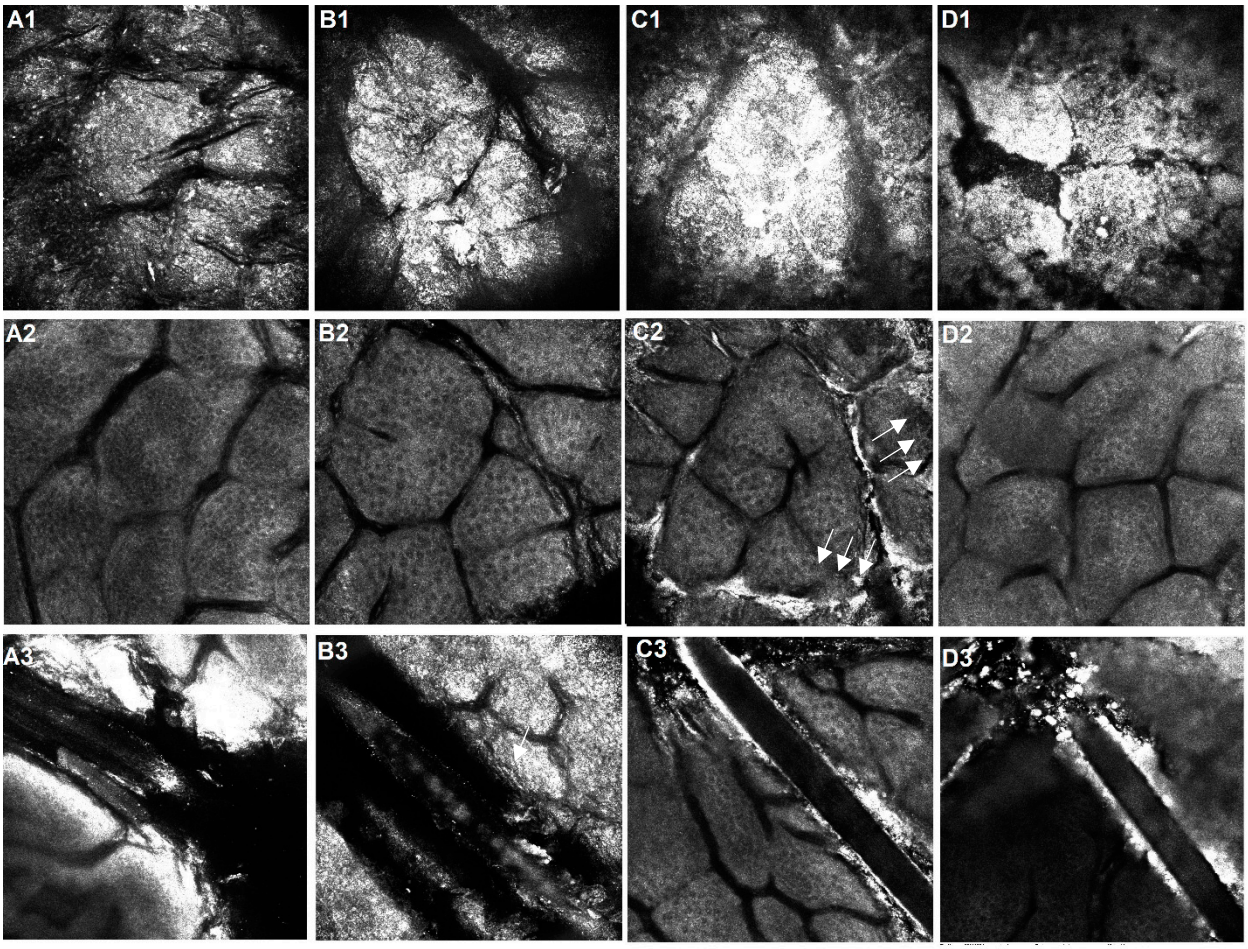

Figure 9. RCM images of the stratum corneum (A1, B1, C1, D1), granular layer (A2, B2, C2, D2) and hair/hair follicle (A3, B3, C3, D3) of the porcine.

A: Non treated Control; B: Vehicle, C: formulation containing the coated ZnOn, D: formulation containing the uncoated ZnOn

The increased reflectance in the skin treated with the formulation containing the coated ZnOn was observed only in the skin furrows and hair follicles, but not within the keratinocytes, which could suggest that the nanoparticles did not enter the cells. In addition, the honeycomb pattern was maintained in the skins treated with the formulations and there were no signs of inflammation in 12 hours. However, it is possible that the penetration was underestimated for the skins treated with the formulation containing the uncoated ZnOn. These nanoparticles did not have a protective cover and the zinc ions could have been liberated from the ZnOn accumulated on the stratum corneum, promoted by the hydrolysis of ZnOn to Zn^{2+} at the normal acidic pH of the skin (5).

For many years, the penetration of topically applied substances through the stratum corneum was assumed to be diffusion inside the lipid layers surrounding the corneocytes. In the last decade, investigations attributed that the hair follicles perform a significant part in skin penetration (36). Moreover, studies have shown that nanoparticles accumulated in hair follicles can remain in the follicles for up to 10 days until gradually cleared by sebum flow (36). Hair follicle stem cells play vital roles in the hair cycle and skin regeneration after injury. ZnOn that accumulated in hair follicles have been shown to impair the transcriptional activity of genes important for hair follicle stem cells differentiation and increased the expression of apoptosis-related proteins. The pathways involved in

cellular communication, cell differentiation, and RNA biosynthesis were also altered (12). A recent study using Franz diffusion cell showed that ZnOn accumulated on the skin surface and within the skin furrows but did not enter or cause cellular toxicity in the viable epidermis, however zinc ion concentrations in the viable epidermis of excised human skin were slightly elevated (5).

The protocol used in this study employed one application of the formulations. The formulations accumulated on the skin furrows, hair and hair follicle; however, it is evident that repeated daily application of ZnOn may lead to an increase in the concentration of zinc species in the skin (5). Therefore, to clarify the safety concerns, biochemical markers of oxidative stress and inflammation should be assessed after prolonged use of formulations containing ZnOn.

4. Conclusion

The size distribution and morphology of the nanoparticles were similar to what was previously described in the literature; however, in this study dynamic light scattering was found an appropriate technique to measure the hydrodynamic diameter of the coated ZnOn in ethyl acetate.

Aggregates were the smallest particles found in the developed formulations, and the incorporation of ZnOn led to formulations more consistent and easier to spread. Although the micrographs presented instability signs for the formulations containing the uncoated and coated ZnOn at 60 and 90 days, respectively, the rheological assessment indicated that the formulations were stable for 30 days at 45ºC.

The assessment off the skin penetration by reflectance confocal laser microscopy indicated that the formulations did not permeate into the deepest layers of the skin, but accumulated on the skin furrows, hair and hair follicle. However, it is evident that repeated daily application of ZnOn may lead to an increase in the concentration of zinc species in the skin. Therefore, to clarify the safety concerns, biochemical markers of oxidative stress and inflammation should be assessed after prolonged use of formulations containing ZnOn.

Supplementary Materials: The following supporting information can be downloaded at the website of this paper posted on Preprints.org.

Acknowledgments: The authors are grateful to the Conselho Nacional de Desenvolvimento Científico e Tecnológico (CNPq) and the Fundação de Amparo a Pesquisa do Estado de São Paulo (FAPESP). This study was financed in part by the Coordenação de Aperfeiçoamento de Pessoal de Nível Superior - Brasil (CAPES) - Finance Code 001. The authors are thankful to Malvern Panalytical, especially to Henrique Kajiyama and Wagner Vitalis for providing the DIP CELL kit.

Conflicts of Interest: The authors have no conflict of interest to declare.

Abbreviations

ZnOn: Zinc Oxide nanoparticles

References

1. Albanese A, Tang PS, Chan WC. The effect of nanoparticle size, shape, and surface chemistry on biological systems. Annual review of biomedical engineering. 2012;14:1-16. doi: 10.1146/annurev-bioeng-071811-150124.
2. Jose J, Netto G. Role of solid lipid nanoparticles as photoprotective agents in cosmetics. Journal of cosmetic dermatology. 2018. doi: 10.1111/jocd.12504.
3. Chen LL, Wang SQ. Chapter 18 - Nanotechnology in Photoprotection. In: Hamblin MR, Avci P, Prow TW, editors. Nanoscience in Dermatology. Boston: Academic Press; 2016. p. 229-36.
4. Cross SE, Innes B, Roberts MS, Tsuzuki T, Robertson TA, McCormick P. Human Skin Penetration of Sunscreen Nanoparticles: In-vitro Assessment of a Novel Micronized Zinc Oxide Formulation. Skin Pharmacology and Physiology. 2007;20(3):148-54. doi: 10.1159/000098701.
5. Mohammed YH, Holmes A, Haridass IN, Sanchez WY, Studier H, Grice JE, et al. Support for the Safe Use of Zinc Oxide Nanoparticle Sunscreens: Lack of Skin Penetration or Cellular Toxicity after Repeated Application in Volunteers. Journal of Investigative Dermatology. 2019;139(2):308-15. doi: https://doi.org/10.1016/j.jid.2018.08.024.

6. Kocbek P, Teskač K, Kreft ME, Kristl J. Toxicological Aspects of Long-Term Treatment of Keratinocytes with ZnO and TiO2 Nanoparticles. Small. 2010;6(17):1908-17. doi: 10.1002/smll.201000032.
7. Sharma V, Shukla RK, Saxena N, Parmar D, Das M, Dhawan A. DNA damaging potential of zinc oxide nanoparticles in human epidermal cells. Toxicology Letters. 2009;185(3):211-8. doi: https://doi.org/10.1016/j.toxlet.2009.01.008.
8. Patzelt A, Knorr F, Blume-Peytavi U, Sterry W, Lademann J. Hair follicles, their disorders and their opportunities. Drug Discovery Today: Disease Mechanisms. 2008;5(2):e173-e81. doi: https://doi.org/10.1016/j.ddmec.2008.04.006.
9. Lu J, Guo J-H, Tu X-L, Zhang C, Zhao M, Zhang Q-W, et al. Tiron Inhibits UVB-induced AP-1 binding sites transcriptional activation on MMP-1 and MMP-3 promoters by MAPK signaling pathway in human dermal fibroblasts. PloS one. 2016;11(8):e0159998.
10. Yin H, Coleman VA, Casey PS, Angel B, Catchpoole HJ, Waddington L, et al. A comparative study of the physical and chemical properties of nano-sized ZnO particles from multiple batches of three commercial products. Journal of Nanoparticle Research. 2015;17(2):96. doi: 10.1007/s11051-014-2851-y.
11. Singh M, Kapoor A, Bhatnagar A. Oxidative and reductive metabolism of lipid-peroxidation derived carbonyls. Chemico-Biological Interactions. 2015;234(Supplement C):261-73. doi: https://doi.org/10.1016/j.cbi.2014.12.028.
12. Ge W, Zhao Y, Lai F-N, Liu J-C, Sun Y-C, Wang J-J, et al. Cutaneous applied nano-ZnO reduce the ability of hair follicle stem cells to differentiate. Nanotoxicology. 2017;11(4):465-74. doi: 10.1080/17435390.2017.1310947.
13. Leite-Silva VR, Liu DC, Sanchez WY, Studier H, Mohammed YH, Holmes A, et al. Effect of flexing and massage on in vivo human skin penetration and toxicity of zinc oxide nanoparticles. Nanomedicine (London, England). 2016;11(10):1193-205. doi: 10.2217/nnm-2016-0010.
14. Leite-Silva VR, Sanchez WY, Studier H, Liu DC, Mohammed YH, Holmes AM, et al. Human skin penetration and local effects of topical nano zinc oxide after occlusion and barrier impairment. European Journal of Pharmaceutics and Biopharmaceutics. 2016;104:140-7. doi: https://doi.org/10.1016/j.ejpb.2016.04.022.
15. Holmes AM, Song Z, Moghimi HR, Roberts MS. Relative Penetration of Zinc Oxide and Zinc Ions into Human Skin after Application of Different Zinc Oxide Formulations. ACS nano. 2016;10(2):1810-9. doi: 10.1021/acsnano.5b04148.
16. Lu PJ, Cheng WL, Huang SC, Chen YP, Chou HK, Cheng HF. Characterizing titanium dioxide and zinc oxide nanoparticles in sunscreen spray. International Journal of Cosmetic Science. 2015;37(6):620-6. doi: 10.1111/ics.12239.
17. Lu P-J, Huang S-C, Chen Y-P, Chiueh L-C, Shih DY-C. Analysis of titanium dioxide and zinc oxide nanoparticles in cosmetics. Journal of Food and Drug Analysis. 2015;23(3):587-94. doi: https://doi.org/10.1016/j.jfda.2015.02.009.
18. Singh C, Friedrichs S, Levin M, Birkedal R, Jensen K, Pojana G, et al. NM-series of representative manufactured nanomaterials: Zinc oxide NM-110, NM-111, NM-112, NM-113 characterisation and test item preparation. EUR 25066 EN-2011. 2011.
19. Calixto LS, Maia Campos P. Physical-Mechanical characterization of cosmetic formulations and correlation between instrumental measurements and sensorial properties. Int J Cosmet Sci. 2017;39(5):527-34. doi: 10.1111/ics.12406.
20. United States Pharmacopeia (USP). Microbiological Tests. 2017;40:117-30.
21. Pleus R. Nanotechnologies-Guidance on Physicochemical Characterization of Engineered Nanoscale Materials for Toxicologic Assessment. ISO: Geneva, Switzerland. 2012.
22. Irfan M, Moniruzzaman M, Ahmad T, Mandal PC, Bhattacharjee S, Abdullah B. Ionic liquid based extraction of flavonoids from Elaeis guineensis leaves and their applications for gold nanoparticles synthesis. Journal of Molecular Liquids. 2017;241:270-8. doi: https://doi.org/10.1016/j.molliq.2017.05.151.
23. Berg JM, Romoser A, Banerjee N, Zebda R, Sayes CM. The relationship between pH and zeta potential of~ 30 nm metal oxide nanoparticle suspensions relevant to in vitro toxicological evaluations. Nanotoxicology. 2009;3(4):276-83.
24. Leite-Silva VR, Le Lamer M, Sanchez WY, Liu DC, Sanchez WH, Morrow I, et al. The effect of formulation on the penetration of coated and uncoated zinc oxide nanoparticles into the viable epidermis of human skin in vivo. European journal of pharmaceutics and biopharmaceutics : official journal of Arbeitsgemeinschaft fur Pharmazeutische Verfahrenstechnik eV. 2013;84(2):297-308. doi: 10.1016/j.ejpb.2013.01.020.
25. Dai S, Jiang F, Corke H, Shah NP. Physicochemical and textural properties of mozzarella cheese made with konjac glucomannan as a fat replacer. Food research international (Ottawa, Ont). 2018;107:691-9. doi: 10.1016/j.foodres.2018.02.069.
26. Shakerardekani A, Karim R, Ghazali HM, Chin NL. Development of Pistachio (Pistacia vera L.) spread. Journal of food science. 2013;78(3):S484-9. doi: 10.1111/1750-3841.12045.

27. Tamburic S, Sisson H, Cunningham N, Stevic M. Rheological and texture analysis methods for quantifying yield value and level of thixotropy. SOFW Journal. 2017;143:24-30.
28. Gaspar LR, Maia Campos PM. Rheological behavior and the SPF of sunscreens. Int J Pharm. 2003;250(1):35-44.
29. RADOČAJ O, DIMIĆ E, Diosady LL, VUJASINOVIĆ V. Optimizing the texture attributes of a fat-based spread using instrumental measurements. Journal of Texture Studies. 2011;42(5):394-403.
30. Gilbert L, Savary G, Grisel M, Picard C. Predicting sensory texture properties of cosmetic emulsions by physical measurements. Chemometrics and Intelligent Laboratory Systems. 2013;124:21-31. doi: https://doi.org/10.1016/j.chemolab.2013.03.002.
31. Camargo Junior FB. Desenvolvimento de formulações cosméticas contendo pantenol e avaliação dos seus efeitos hidratantes na pele humana por bioengenharia cutânea: Universidade de São Paulo; 2006.
32. Martin A, Bustamante P, Chun AHC. Rheology. Physical Pharmacy, Philadelphia: Lea & Febiger, cap. 17, p. 453-473; 1993.
33. Leonardi G, Maia Campos P. Estabilidade de formulações cosméticas. International Journal of Pharmaceutical Compounding. 2001;3(4):154-6.
34. Rajadhyaksha M, Marghoob A, Rossi A, Halpern AC, Nehal KS. Reflectance confocal microscopy of skin in vivo: From bench to bedside. Lasers in Surgery and Medicine. 2017;49(1):7-19. doi: 10.1002/lsm.22600.
35. Patzelt A, Richter H, Knorr F, Schäfer U, Lehr C-M, Dähne L, et al. Selective follicular targeting by modification of the particle sizes. Journal of Controlled Release. 2011;150(1):45-8. doi: https://doi.org/10.1016/j.jconrel.2010.11.015.
36. Lademann J, Richter H, Teichmann A, Otberg N, Blume-Peytavi U, Luengo J, et al. Nanoparticles – An efficient carrier for drug delivery into the hair follicles. European Journal of Pharmaceutics and Biopharmaceutics. 2007;66(2):159-64. doi: https://doi.org/10.1016/j.ejpb.2006.10.019.